Research Article
https://doi.org/10.1631/jzus.B2500818

Supplemental sodium butyrate improves uterine environment for embryo implantation in mammals

Yuwen CHEN[1], Xiaojian XU[1], Zhenhong YAN[1], Qianhong YE[2]✉, Xianghua YAN[1,3]✉

[1]*National Key Laboratory of Agricultural Microbiology, Hubei Hongshan Laboratory, Frontiers Science Center for Animal Breeding and Sustainable Production, Hubei Provincial Engineering Laboratory for Pig Precision Feeding and Feed Safety, College of Animal Science and Technology, Huazhong Agricultural University, Wuhan 430070, China*
[2]*College of Food Sciences and Technology, Huazhong Agricultural University, Wuhan 430070, China*
[3]*China National Engineering Research Center for Green Feed and Healthy Breeding, Key Laboratory of Animal Molecular Nutrition, Ministry of Education, Key Laboratory of Animal Nutrition and Feed Science (Eastern of China), Ministry of Agriculture and Rural Affairs, Zhejiang Key Laboratory of Nutrition and Breeding for High-quality Animal Products Institute of Feed Science, College of Animal Science, Zhejiang University, Hangzhou 310058, China*

Abstract: Background: Embryo mortality during early gestation limits litter size in swine. Sodium butyrate (SB) is a potential feed additive for improving gut health and productivity. Objective: To evaluate the effects of SB supplementation during early gestation on reproductive performance in sows and mice. Methods: In the sow trial, gestating sows were fed diets supplemented with 0% (Ctrl), 0.05% (LSB), 0.10% (MSB), or 0.20% (HSB) SB from gestation day (GD) 1 to 28. Fecal samples (GD14 and GD28) underwent 16S rRNA sequencing and metabolomics. Litter performance was recorded at farrowing. In the mouse trial, identical SB doses were given from GD1 to GD6. Implantation sites were counted on GD6, and uterine tissues were subjected to transcriptomics and proteomics. Colonic content and serum were analyzed by 16S rRNA sequencing and metabolomics. Results: In sows, the LSB group exhibited significant increases in total litter size, live litter size, and healthy litter size compared to the Ctrl group. Similarly, in mice, SB supplementation significantly increased the number of embryo implantation sites. Integrated multi-omics in mice revealed that SB reshaped the gut microbiota (enriching *Lactobacillus* and *Bifidobacterium*) and colonic metabolome, upregulating uterine endometrial receptivity-related genes (*Wnt4* and *H19*). Conclusions: SB supplementation is associated with alterations in the gut microbiota, serum metabolome, and uterine transcriptome/proteome, suggesting a potential link between these compartments that may contribute to improved embryo implantation. SB represents a promising nutritional strategy to improve reproductive efficiency in swine and potentially other mammals.

Key words: Sodium butyrate; Embryo implantation; Endometrial receptivity; Gut microbiota; Metabolome; Multi-omics

✉Xianghua YAN, xhyan2024@zju.edu.cn
Qianhong YE, qianhye@mail.hzau.edu.cn
Xianghua YAN, https://orcid.org/0000-0003-2238-6218
Qianhong YE, https://orcid.org/0009-0002-7826-5458
Yuwen CHEN, https://orcid.org/0009-0005-0137-7584

Received Dec. 12, 2025; Revision accepted May 13 2026;
Crosschecked xxx. xx, xxxx

1 Introduction

A fundamental challenge in modern animal agriculture, particularly in intensive swine production, is the significant gap between ovulation rate and the number of live litter. This loss, occurring predominantly during early gestation, represents a major economic inefficiency, limiting the genetic potential and profitability of breeding herds. In swine, the loss is even more pronounced during the peri-implantation period. Genetic selection programs over 14 generations successfully increased ovulation rate and the number of fetuses at 50 d of gestation, yet the correlated increase in the number of fully formed and live-born pigs was proportionally smaller, highlighting the bottleneck of embryonic and fetal survival. This gap between conception potential and realized offspring underscores the critical need to understand and manage the uterine environment and maternal physiology to support embryonic development (Johnson et al., 1999). These losses are concentrated across critical developmental windows, including the pre-elongation phase, trophoblastic elongation, and the peri-attachment period (Dey et al., 2004). Therefore, developing effective interventions, such as nutritional strategies (Kimura et al., 2020), to reduce early pregnancy loss and enhance implantation efficiency is of profound clinical and economic significance. Maternal diet composition and nutrient intake significantly influence embryo quality and offspring development. For instance, dietary fatty acid levels influence fatty acid profiles in serum, ovarian and uterine tissues, thereby shaping the local metabolic environment that regulates follicular and embryonic development (Zhao et al., 2021).

A successful pregnancy hinges on the establishment of endometrial receptivity, a transient implantation period, also known as the endometrial receptivity window, during which the uterus is receptive to blastocyst attachment. This critical period occurs on days 5-9 post-ovulation in humans, on gestation day (GD) 4.5-5.0 in mice, and on GD9.0-13.0 in swine (Achache et al., 2006; Paria et al., 1993; Ye et al., 2003). The implantation process itself is a highly coordinated dialogue between the blastocyst trophectoderm and the maternal endometrium, canonically divided into three phases: apposition, adhesion, and invasion (Wang et al., 2006; Red-Horse et al., 2004; Zhang et al., 2012). The success of this process is governed by multiple factors, including embryonic developmental competence (Keefe et al., 2015), endometrial receptivity (Ye et al., 2005), a meticulous balance of maternal estrogen and progesterone (Dey et al., 2004), and a tolerogenic local immune microenvironment (Munoz-Suano et al., 2011). The maternal immune system must also achieve a delicate balance, tolerating the semi-allogeneic embryo while maintaining defense against pathogens. Dysregulation in any of these components can lead to implantation failure and pregnancy loss.

Maternal nutrition is a cornerstone for optimizing reproductive outcomes. Previous research has focused mainly on polyunsaturated fatty acids (PUFAs), with higher intake of specific n-3 PUFAs being associated with improved reproductive outcomes (Mumford et al., 2016). However, the effects of short chain fatty acids (SCFAs) on embryo implantation and reproductive success remain relatively unexplored (Yamada et al., 2012). SCFAs, produced mainly by gut microbial fermentation of dietary fiber, are key metabolic mediators of host physiology (Dalile et al., 2019). Among SCFAs, sodium butyrate (SB) is widely recognized for its anti-inflammatory and antioxidant properties and has been used as a feed additive in livestock production. Once ingested, it dissociates into butyrate ions, which serve as a primary energy substrate for colonic epithelial cells. This metabolic substrate contributes to the regulation of epithelial growth and repair, enhances tight junction integrity, and combats oxidative stress through molecular pathways like histone deacetylase (HDAC) inhibition (Dou et al., 2020). Additionally, butyrate has anti-inflammatory properties, suppressing the nuclear factor kappa B (NF-κB) pathway and reducing pro-inflammatory cytokines, such as tumor necrosis factor-alpha (TNF-α) and interleukin-6 (IL-6) (de Lazari et al., 2020).

Functionally, SB is a primary energy source for colonocytes, contributing to gut barrier integrity (Koh et al., 2016). It also exerts immunomodulatory effects, for instance, by suppressing the NF-κB pathway (Quivy et al., 2004). In the context of reproduction, dietary SB supplementation during mid-to-late gestation in sows has been shown to improve reproductive performance (Lu et al., 2025). Moreover, SB can enhance the developmental competence of porcine oocytes in vitro (Lin et al., 2014).

Despite these findings, research has largely overlooked the impact of SB during early gestation—the very

period when embryonic losses are highest. The underlying mechanisms remain elusive: does SB act by modulating the maternal uterine environment or by directly enhancing embryonic quality? It is hypothesized that gut-derived metabolites, such as SCFAs, can reach the embryo and influence its development (Kimura et al., 2020). Therefore, building upon our prior work (Ye et al., 2019), this study investigated the effects of dietary SB supplementation during early gestation on reproductive performance in sows and mice. Using an integrated multi-omics approach, we sought to identify correlational links, specifically examining whether alterations associated with SB in the gut microbiota correlate with embryo implantation.

2 Materials and methods

2.1 Feces collection from sows

All procedures involving animals were approved by the Animal Subjects Committee of Huazhong Agricultural University (HZAUSW-2023-0064). From GD 1 to 28, 214 Landrace×Yorkshire crossbred (L×Y) sows were housed in individual stalls and fed a basal corn-soybean meal diet (2.2 kg/day) meeting NRC standards. Following our group's prior research, the diet was supplemented with four inclusion levels of SB: 0% (Ctrl), 0.05% (LSB), 0.10% (MSB), and 0.20% (HSB). The ingredient and nutrient composition of the diet is presented in Table 1. Fresh fecal samples were collected on the morning of GD14 and GD28 into sterile centrifuge tubes and immediately snap-frozen in liquid nitrogen.

Table 1 Ingredients and nutrients composition of the diet used in this trial (air-dry basis)

Items	Pregnancy Phase
Ingredients (%)	
Corn	33.80
Soybean oil	1.00
Wheat	15.00
43% Soybean meal	6.00
Wheat bran	23.00
Rice bran meal	12.00
Fermented feed[1]	5.00
Pregnancy premix[2]	4.00
Baocikang[3]	0.20
Total	100.00
Nutrient composition	
Digestive energy (MJ/kg)	2.965
Lys (%)	0.92
Met + Cys (%)	0.64
Available phosphorus (%)	0.79
Calcium (%)	0.72
Crude protein (%)	13.60

1) Fermented feed ingredients consist of soybean meal, corn, wheat bran, etc., with moisture content≥42.0%, crude protein (dry basis)≥15%, total acidity≥1.5%, acid-soluble protein (as % of CP)≥12.0%, and pH≤5.0.

2) Composition of Pregnancy Premix: Rice Bran Meal 13.65%, Sodium Chloride 10.00%, Calcium Hydrogen Phosphate 32.50%, Limestone Powder 25.00%, Glycine Iron Complex 0.75%, yeast selenium 0.25%, zinc methionine complex 0.50%, breeding pig multivitamins 0.80%, pig trace mineral premix 2.50%, choline chloride 3.00%, heat-stable phytase 0.50%, Lysine 4.00%, Methionine 1.00%, Threonine 1.20%, Vitamin E 50% 0.25%, Chromium Picolinate 0.25%, Encapsulated Vitamin C 0.75%, Wheat Complex Enzymes 0.50%, Intestinal Health Acid 2.50%, D-Biotin 2% 0.10%.

3) Baocikang is a Bacillus subtilis preparation with live bacteria content≥1.0×10⁸ CFU/g.

2.2 Sample collection in mice

All procedures involving animals were approved by the Animal Subjects Committee of Huazhong Agricultural University (HZAUMO-2025-0282). ICR mice (7 weeks old, 30.73±0.18 g) were housed in a temperature-controlled environment (22-25 °C) on a 12-h-light/12-h-dark cycle with ad libitum access to feed

and water. After 1 week of acclimatization, 45 virgin female mice were mated with males (1:2 ratio). The morning on which a vaginal plug was detected was designated as GD1. At GD6, mice were euthanized. Blood was collected, and serum was obtained by centrifugation (3,000×g, 15 min, 4 °C) and stored at -80 °C. Uterine horns were excised, rinsed, and snap-frozen. Colonic contents were collected and immediately snap-frozen.

2.3 Microbial DNA extraction and 16S rRNA gene sequencing

Total microbial DNA was extracted using the E.Z.N.A.® soil DNA Kit (Omega Bio-tek, Norcross, GA, U.S.) according to the manufacturer's instructions. The V3–V4 hypervariable region of the 16S rRNA gene was amplified with primer pairs 338F (5'-ACTCCTACGGGAGGCAGCAG-3') and 806R(5'-GGACTACHVGGGTWTCTAAT-3') for swine samples, and the near-full-length 16S rRNA gene was amplified with primer pairs 27F (5'-AGAGTTTGATCCTGGCTCAG-3') and 1492R (5'-GGTTACCTTGTTACGACTT-3') for mouse samples. Amplicons were sequenced on an Illumina MiSeq PE300 platform. Sequence data were processed using the Qiime2 pipeline with the DADA2 plugin for amplicon sequence variant (ASV) calling.

16S rRNA gene sequencing was used to characterize the taxonomic composition of the gut microbiota, as it is a cost-effective and robust method for assessing community structure. While shotgun metagenomics could provide additional insights into functional gene content, our primary objective was to identify compositional shifts. The functional output of the microbiota was directly assessed through non-targeted and targeted metabolomics of fecal and serum samples, which captures the net metabolic activity of the microbial community.

2.4 Untargeted metabolomic analysis

For solid samples, 50 mg of sample was extracted with 400 μL methanol:water (4:1, v/v) containing 0.02 mg/mL L-2-chlorophenylalanine as internal standard. The mixture was ground, ultrasonicated, kept at −20 °C, and centrifuged. For liquid samples, 100 μL was mixed with 400 μL acetonitrile:methanol (1:1, v/v) containing the same internal standard, then vortexed, ultrasonicated, precipitated at −20 °C, and centrifuged; the supernatant was dried, reconstituted, and centrifuged again (Ye et al., 2025).

LC-MS/MS analysis was performed with a Thermo UHPLC-Exploris 240 system equipped with an ACQUITY HSS T3 column (100×2.1 mm, 1.8 μm). Mobile phases were 0.1% formic acid in water:acetonitrile (95:5) (A) and in acetonitrile:isopropanol:water (47.5:47.5:5) (B) at 0.40 mL/min and 40 °C with gradient elution. Electrospray ionization (ESI) was performed in positive and negative modes, with full MS resolution set to 60,000, MS/MS resolution to 15,000, and the mass range from 70 to 1050 m/z. After data acquisition, raw data were processed using Progenesis QI (Waters Corporation, Milford, USA) for peak detection, extraction, alignment, and integration.

To minimize errors, features with >20% missing values within any group were removed. Subsequently, missing values were imputed using the minimum value across all samples. The areas of mass spectral peaks were normalized by sum normalization. Features with a relative standard deviation (RSD) of >30% in quality control (QC) samples were also excluded. The data were then subjected to log10 transformation, yielding the final data matrix for subsequent analyses.

Initial metabolite annotation was performed by matching mass spectral data against the HMDB database (http://www.hmdb.ca/), the Metlin database (https://metlin.scripps.edu/), and a proprietary in-house library established by Majorbio. This annotation was applied uniformly to both serum and fecal samples.

Multivariate statistical analyses, including principal component analysis (PCA) and partial least squares discriminant analysis (PLS-DA), were performed using the ropls package (Version 1.6.2) in R. For pathway enrichment analysis, the putatively identified metabolites were further annotated against the Kyoto Encyclopedia of Genes and Genomes (KEGG) databases (https://www.kegg.jp/kegg/pathway.html), and enrichment analysis was carried out using the scipy.stats package in Python. The data were analyzed using the free online majorbio cloud platform (cloud.majorbio.com) (Ren et al., 2022).

2.5 Quantification of SCFAs

SCFAs in feces were quantified with gas chromatography. Briefly, 1 g of feces were weighed, dissolved and homogenized in 1 mL methanol. Then, the homogenized solution was centrifuged at 12,000×g for 10 min at 4 °C to obtain the supernatant which was then transferred into a new tube. The supernatant was diluted (5:1, v/v) with 25% metaphosphoric acid at 4 °C overnight and then centrifuged at 12,000×g for 10 min at 4 °C. Finally, the SCFA content of the supernatant was analyzed using gas chromatography, following a previously published protocol (Fellows et al., 2018).

SCFAs in sow diets were determined using a DIONEX 2500 ion chromatography system. Silage samples (25 g) were extracted with 225 mL deionized water at 4 °C for 24 h. The extract was filtered through a 0.45-μm membrane. Ion chromatography was performed on a Dionex IonPac AS11 column (250×4.6 mm) with 1% KOH as mobile phase at 0.8 mL/min. Injection volume was 10 μL and detection was by conductivity. Lactic, acetic, propionic and butyric acids were quantified using external calibration. The method showed good linearity (R^2>0.999), low RSDs (<2%), and recoveries between 97.5% and 99.8% (Jia et al., 2016).

2.6 Transcriptome analysis

Total RNA was extracted from frozen uterine tissues using TRIzol reagent (Invitrogen). RNA integrity was verified using an Agilent Bioanalyzer (all samples had an RNA Integrity Number, RIN, of >8.0). Libraries were prepared from 1 μg of total RNA using the Illumina Stranded mRNA Prep Kit and sequenced on an Illumina NovaSeq X Plus platform to generate 150-bp paired-end reads. Raw sequencing reads were quality-controlled using FastQC and trimmed with Trimmomatic. The cleaned reads were then aligned to the mouse reference genome (GRCm39) using STAR aligner. Gene-level counts were obtained using featureCounts, and differential gene expression analysis was performed using the DESeq2 package in R. Genes with a P<0.05 and |log2 fold change|>1 were considered significantly differentially expressed.

2.7 Proteomic analysis

Uterine tissues were homogenized, and proteins were extracted using RIPA lysis buffer containing protease inhibitors. The protein concentration was determined using a BCA assay. For quantitative proteomics, 100 μg of protein from each sample was digested with trypsin. Based on peptide quantification results, the peptides were analyzed using a VanquishNeo UHPLC system coupled with an Orbitrap Astral mass spectrometer (Thermo Scientific, USA) at Majorbio Bio-Pharm Technology Co. Ltd. (Shanghai, China). The raw data were processed using Proteome Discoverer software (version 3.0, Thermo Fisher Scientific) and searched against the UniProt Mus musculus database. Proteins with a fold change >1.2 or <0.83 and a P<0.05 were considered differentially expressed.

2.8 Hematoxylin and eosin (H&E) staining

Uterine tissues were fixed in 4% paraformaldehyde for 24 h, dehydrated through a graded ethanol series, cleared in xylene, and embedded in paraffin. Sections were cut at a thickness of 5 μm and mounted on glass slides. After deparaffinization and rehydration, the sections were stained with H&E according to standard protocols. The stained sections were examined under a High-resolution Whole Slide Imaging (WSI) System (TEKSQRAY SQS-40Pro) to evaluate the general histoarchitecture of the endometrium.

2.9 Quantification of uterine Wnt4

The concentration of Wnt4 in uterine tissue was determined using a commercial enzyme-linked immunosorbent assay (ELISA) kit (Jiangsu Meimian Industrial Co., Ltd), according to the manufacturer's instructions. Absorbance was measured with a microplate reader, and Wnt4 concentrations were calculated based on the standard curve.

2.10 Protein-Protein Interaction (PPI) network analysis

To explore functional interactions among the differentially expressed proteins, a PPI network was constructed using the STRING database (https://string-db.org/). The analysis was performed with a medium-confidence interaction score cutoff of >0.4.

2.11 Protein-Protein Interaction (PPI) network analysis

All data are presented as mean±SEM. Statistical analyses were performed and figures were generated using GraphPad Prism (v10.1.2, GraphPad Software, San Diego, CA, USA). Comparisons between two groups were conducted using a two-tailed, unpaired Student's t-test or a Mann-Whitney U test, depending on data distribution. Comparisons among more than two groups were performed using a one-way ANOVA followed by Dunnett's post-hoc test. Spearman's rank correlation coefficient was used for correlation heatmaps, and analyses were performed on the Majorbio Cloud Platform (https://www.majorbio.com/tools) (Han et al., 2024). $P<0.05$ was considered statistically significant.

3 Results

3.1 Effects of SB on reproductive performance and gut microbiota in sows

To evaluate the effects of dietary SB on sow reproductive performance, 214 sows were assigned to four treatment groups from GD1 to GD28 (Fig. 1a). At farrowing, sows in the 0.05% SB (LSB) group exhibited significant increases in litter size, live litter size, and number of healthy litter compared to the control (Ctrl) group (Figs 1b–1d). Analysis of fecal samples collected on GD14 and GD28 showed no significant differences among groups in the concentrations of major SCFAs (acetate, propionate, and butyrate) or in serum steroid hormone levels (estradiol and progesterone) at either time point (Figs 1e–1i).

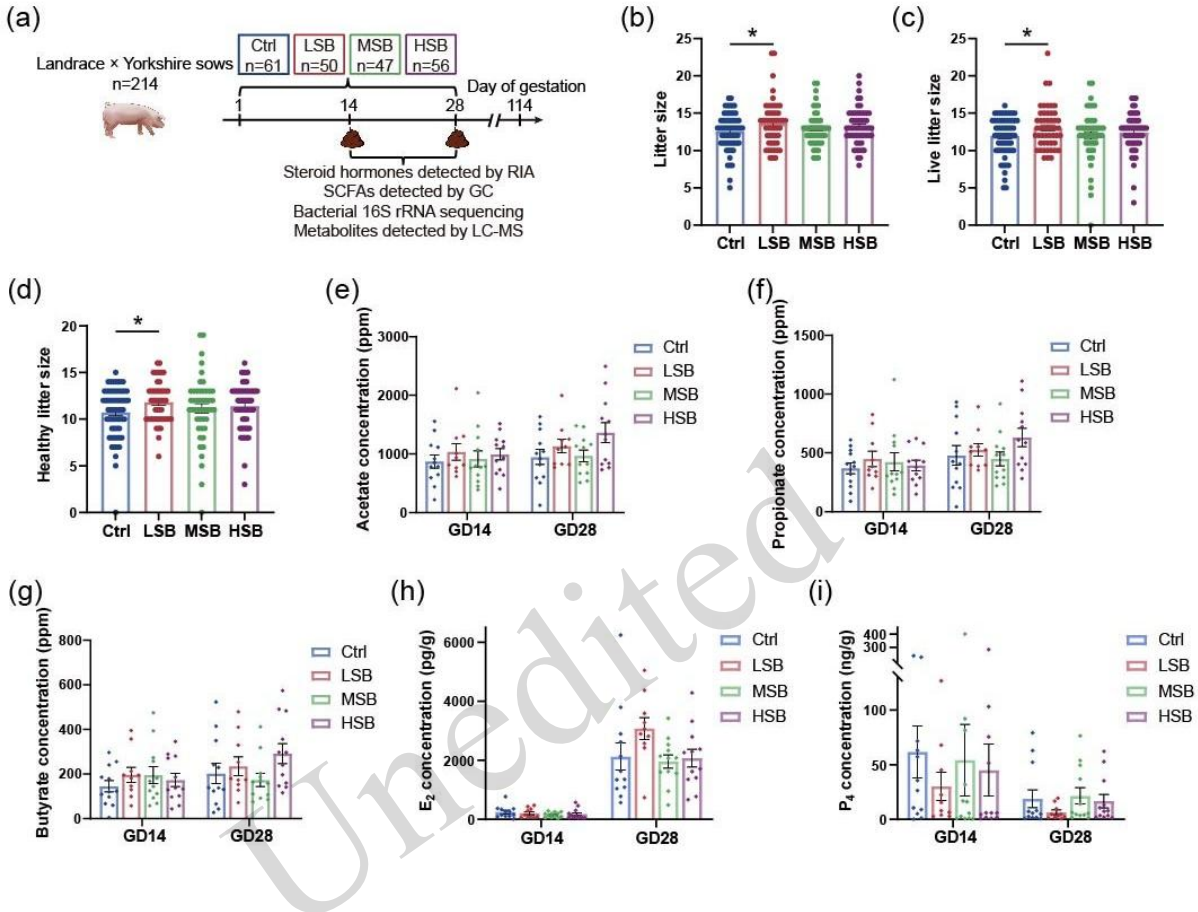

Fig. 1 SB supplementation improves reproductive performance in sows. (a) Overview of study design for unveiling the relationship between maternal colonic microbiota and reproductive performance in sows with diets supplemented with SB. (b–d) Litter size, live litter size and healthy litter size. (e–i) Levels of SCFAs, estradiol (E_2) and progesterone (P_4) in feces of sows at GD14 and GD28. The data are presented as mean±SEM (Ctrl group, n=61; LSB group, n=50; MSB group, n=47; HSB group, n=56). *P<0.05 by Student's t-test. RIA, Radioimmunoassay; GC, Gas chromatography; 16S rRNA, 16S ribosomal RNA; LC-MS, Liquid chromatography-mass spectrometry.

To characterize the associations between SB and the gut microbiota, we performed 16S rRNA gene sequencing. Alpha diversity analysis revealed that in the LSB group on GD14, the Observed species, Chao, Ace, and Shannon index were significantly lower, while the Simpson and Coverage index were significantly higher (Figs 2a–2f). On GD28, there were no significant differences in the Observed species, Chao, Ace, and Shannon index between the two groups, while the Simpson and Coverage index remained elevated in the LSB group (Figs 2g–2l). Beta diversity analysis, visualized by Principal Coordinates Analysis (PCoA), showed no significant separation in the overall microbial community structure between groups on GD14 (P>0.05, Fig. 2m). However, a clear separation emerged by GD28 (P<0.05, Fig. 2n).

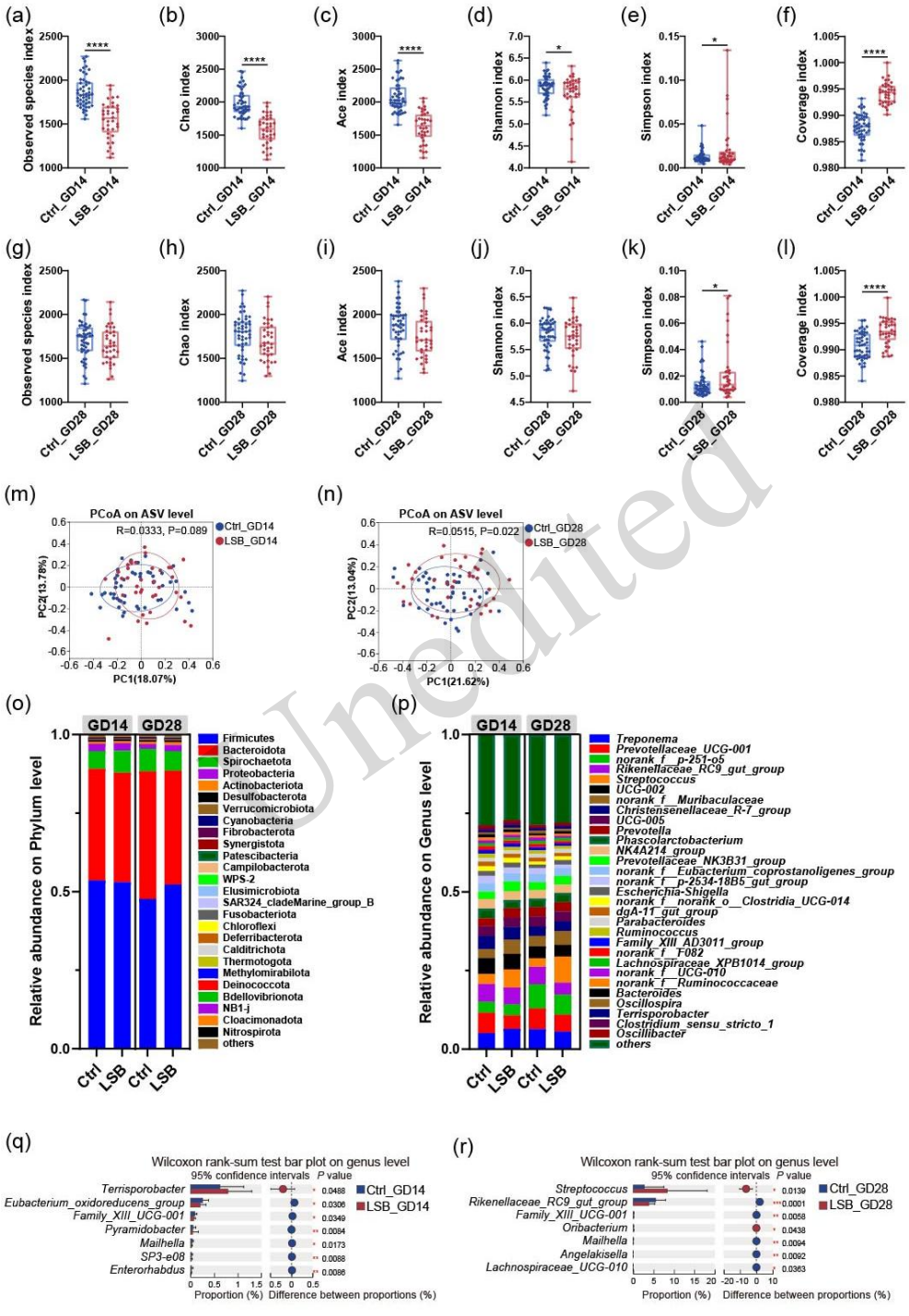

Fig. 2 SB supplementation modulates gut microbiota in sows. (a–l) Alpha diversities of feces bacteria of sows at GD14 and GD28. (m–n) Feces microbial communities clustered using PCoA of weighted Unifrac matrix. (o–p) Microbial composition at the phylum and genus level across the Ctrl and LSB groups on GD14 and GD28. (q–r) Wilcoxon rank-sum test bar plot on genus level. The data are presented as mean±SEM (Ctrl group, n=61; LSB group, n=50; MSB group, n=47; HSB group, n=56). **P*<0.05 and *****P*<0.0001 by Student's *t*-test. PCoA: principal coordinates analysis.

At the phylum level, a significant increase in the relative abundances of Bacteroidota and Spirochaetota were observed in the LSB group on GD14, whereas a significant increase in Firmicutes was found on GD28 (Fig. 2o). At the genus level, the LSB group showed increased relative abundances of *Treponema*, *Streptococcus*, and *Prevotella* at GD14. By GD28, a sustained and specific enrichment of the genus *Streptococcus* was observed in the LSB group compared to the Ctrl group (Fig. 2p). The Wilcoxon rank-sum test revealed that *Terrisporobacter* was significantly enriched in the LSB group on GD14, while *Streptococcus* and *Oribacterium* were significantly enriched on GD28 (Figs 2q and 2r).

3.2 Untargeted metabolomics analysis of SB-induced colonic metabolome alterations of sows

To investigate changes in colonic metabolism, we performed untargeted metabolomic profiling. A total of 2991 metabolites were detected: compared with the Ctrl group, in the LSB group 186 were significantly higher and 164 significantly lower on GD14 (Fig. 3a), and 140 were significantly higher and 134 significantly lower on GD28 (Fig. 3b). The differential metabolites detected in sow feces on GD14 and GD28 are listed in Tables S1 and S2. PLS-DA confirmed a clear separation in the metabolomic profiles between the LSB and Ctrl groups at both time points (Figs 3c and 3d). Differential metabolites on GD14 were enriched mainly in pathways such as sphingolipid metabolism/signaling, neuroactive ligand-receptor interaction, tryptophan metabolism, and regulation of lipolysis in adipocytes (Fig. 3e). On GD28, protein digestion and absorption and mineral absorption were the most prominently enriched pathways (Fig. 3f). A correlation analysis was conducted among the amounts of different colonic metabolites and bacteria, as well as litter size, live litter size and healthy litter size. The results showed that the reproductive performance and amounts of bacteria had a similar correlation pattern to these metabolites (Figs 3g and 3h).

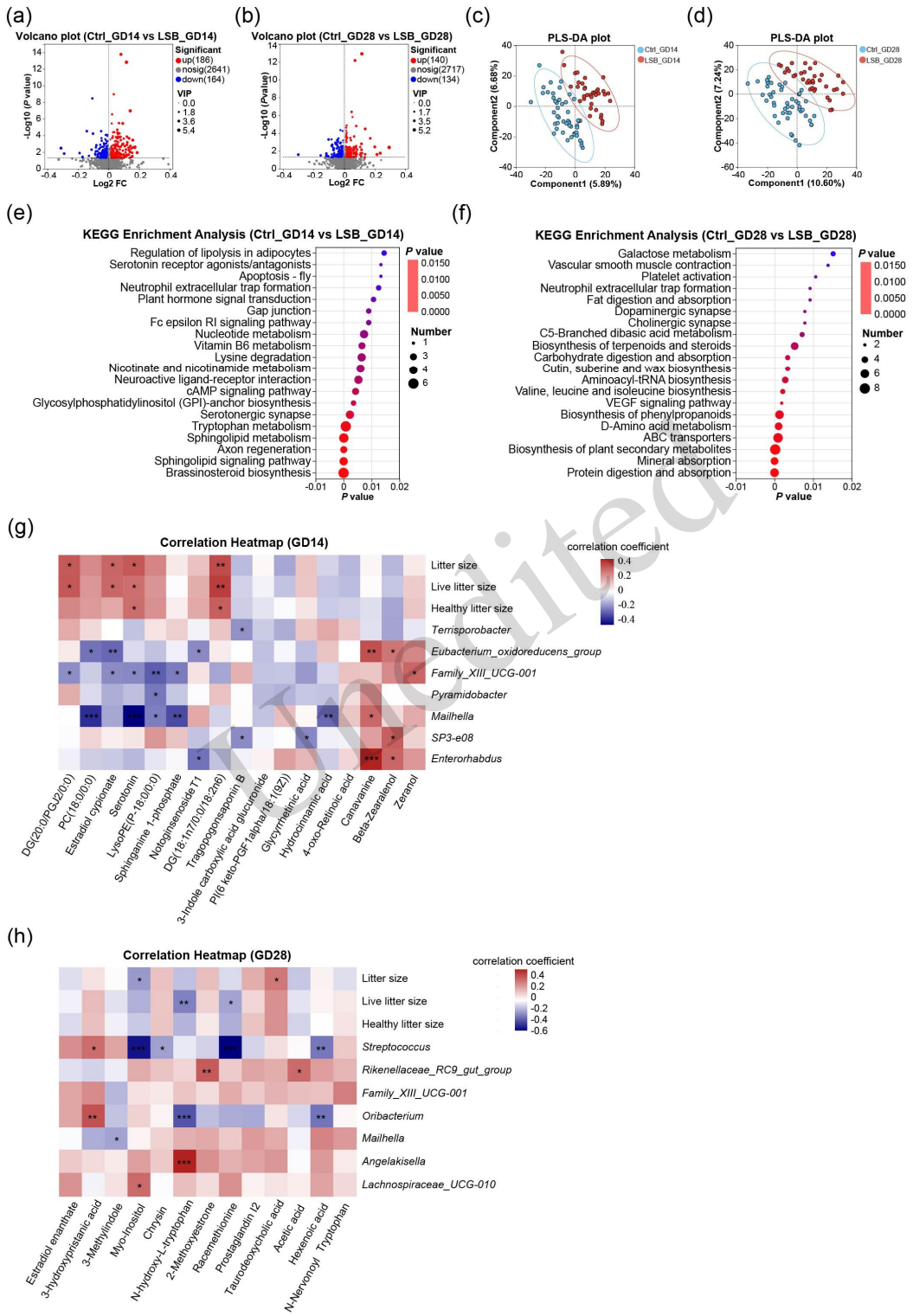

Fig. 3 Untargeted metabolomics analysis reveals SB-induced alterations in the colonic metabolome of sows. (a–b) Volcano plot. (c–d) PLS-DA plot. (e–f) KEGG enrichment analysis. (g–h) Correlating the abundance of up- and down-regulated metabolites with reproductive performance and bacteria. Spearman's correlation coefficient (r) is shown. Red, positive correlation; blue, negative correlation. Color intensity reflects |r|. $P<0.05$ for all displayed correlations. PLS-DA, partial least squares discrimination analysis.

3.3 SB-induced increase in embryo implantation sites in mice

A mouse model was used to further investigate the effects of SB during early gestation, with dietary supplementation from GD1 to GD6 (Fig. 4a). At GD6, the number of embryo implantation sites was significantly increased in the 0.10% SB (MSB) group compared with the Ctrl group (Fig. 4b), as visually indicated by the implantation sites (Fig. 4c). H&E staining revealed well-defined decidual regions with typical morphological features in all groups at GD6 (Fig. 4d). Analysis of the experimental diets confirmed that SB concentrations were consistent with the intended formulations, while levels of other organic acids, such as acetate and propionate, did not differ among groups (Fig. 4e).

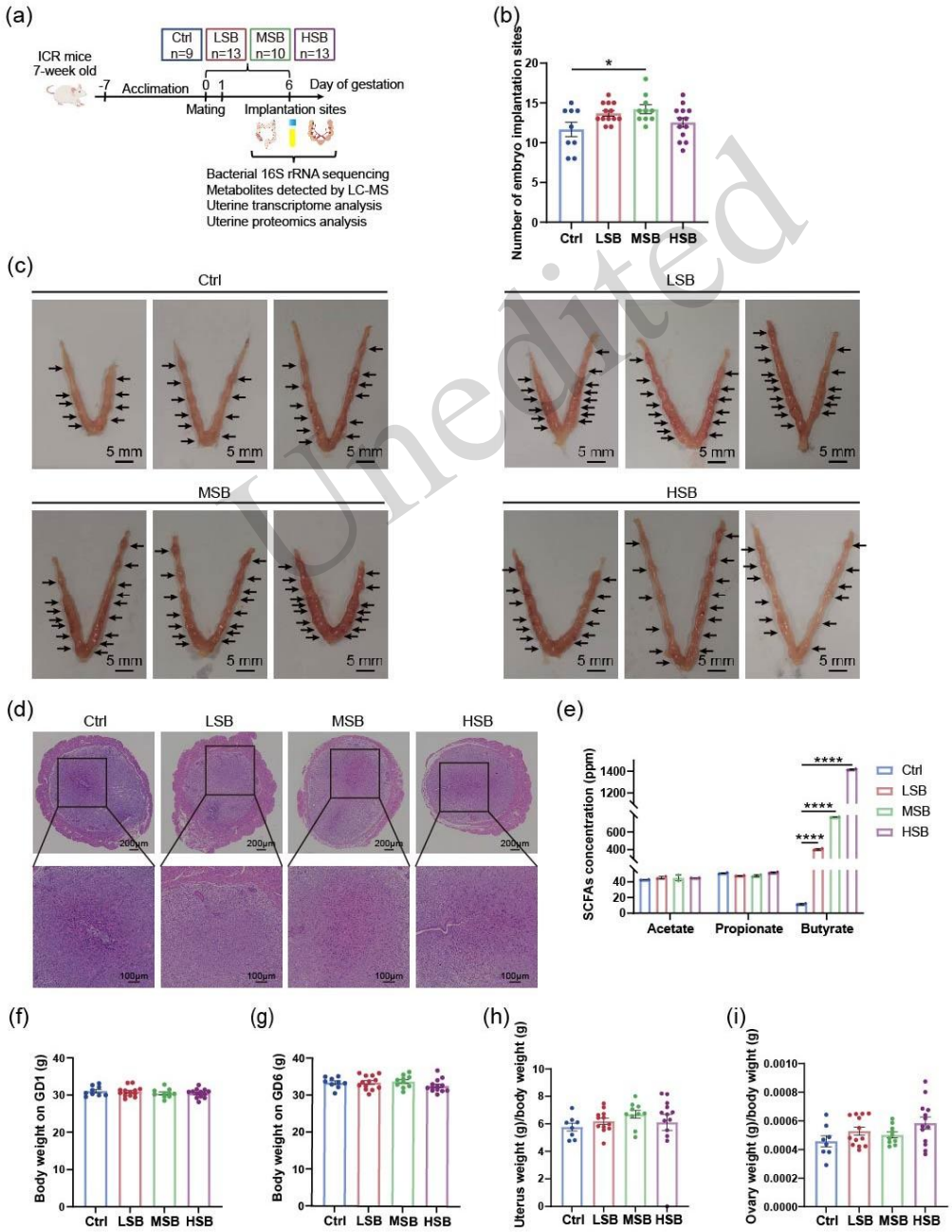

Fig. 4 SB supplementation increases embryo implantation sites in mice. (a) A study design to evaluate the impact of a SB supplemented diet on embryo implantation sites in a mice model. (b) Number of embryo implantation sites at GD6. (c)

Representative morphological images of the embryo implantation sites. (d) Representative H&E stained sections of uterine decidual regions of mice on GD6. (e) Concentrations of acetate, propionate and butyrate in the diet. (f–g) Body weight on GD1 and GD6. (h–i) Uterine weight/body weight and ovarian weight/body weight. The data are presented as mean±SEM (Ctrl group, n=9; LSB group, n=13; MSB group, n=10; HSB group, n=13). **P*<0.05 and *****P*<0.0001 by Student's *t*-test. 16S rRNA, 16S ribosomal RNA; LC-MS, liquid chromatography-mass spectrometry.

No significant differences in maternal body weight were observed among the groups on GD1 (Fig. 4f). While all groups gained weight by GD6, there were no significant differences between them (Fig. 4g). Furthermore, the ratios of uterine weight to body weight and ovarian weight to body weight were comparable across all experimental groups at GD6 (Figs 4h and 4i).

3.4 SB-induced alteration of gut microbiome composition in early gestation mice

We next assessed the impact of SB on the gut microbial community in mice. Alpha diversity analysis revealed a trend toward reduction but did not reach significance in species richness or diversity indices (Observed species, Chao, Ace, Shannon, and Simpson) between the MSB and Ctrl groups (Figs 5a–5e). The sequencing coverage was high and comparable between groups (Fig. 5f). Consistently, beta diversity analysis did not show a significant overall separation in community structure (PCoA, $P>0.05$, Fig. 5g). A Venn diagram (Fig. 5h) shows a substantial number of bacteria shared between groups, with a smaller number of unique bacteria in each. Histological examination of colon biopsies revealed no significant alteration in colonic morphology following dietary SB supplementation (Fig. 5i).

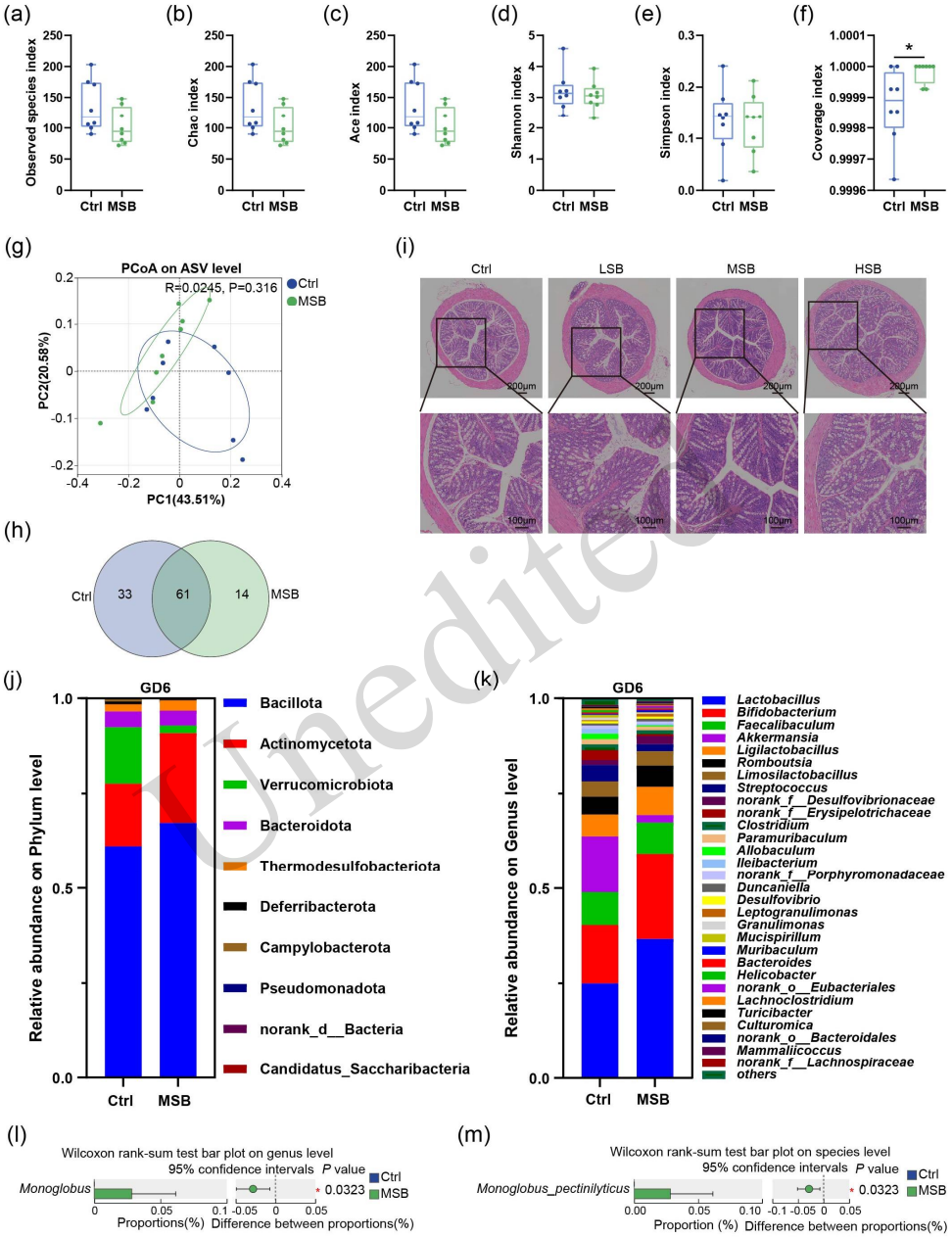

Fig. 5 SB alters the gut microbiome composition in early gestation mice. (a–f) Alpha diversities of colonic bacteria of mice at GD6. (g) Colonic microbial communities clustered using PCoA of weighted Unifrac matrix. (h) Shared and unique genera between Ctrl and MSB groups: a genus level Venn diagram analysis. (i) Representative H&E stained sections of colonic tissue of mice on GD6. (j–k) Microbial composition at the phylum and genus levels across the Ctrl and MSB groups on GD6. (l–m) *M. pectinilyticus* is the significantly enriched taxon in the MSB group. The data are presented as mean±SEM (Ctrl group, n=9; LSB group, n=13; MSB group, n=10; HSB group, n=13). **P*<0.05 by Student's *t*-test. PCoA: principal coordinates analysis.

At the phylum level, the MSB group showed an increased relative abundance of Bacillota and Actinomycetota (Fig. 5j). At the genus level, the relative abundances of *Lactobacillus* and *Bifidobacterium* were higher in the MSB group than in the Ctrl group (Fig. 5k). The Wilcoxon rank-sum test identified the genus *Monoglobus* and the species *M. pectinilyticus* as significantly enriched taxa in the MSB group (Figs 5l and 5m).

3.5 SB-induced gut metabolome alterations and their correlation with implantation success in mice

Untargeted metabolomics of colonic contents identified 54 upregulated and 194 downregulated metabolites in the MSB group compared to the Ctrl group (Fig. 6a). Putative differential metabolites in mouse colonic contents are shown in Table S3. PLS-DA analysis showed a clear separation between the two groups (Fig. 6b). KEGG pathway enrichment analysis of the differential metabolites revealed that arginine biosynthesis was significantly enriched (Fig. 6c).

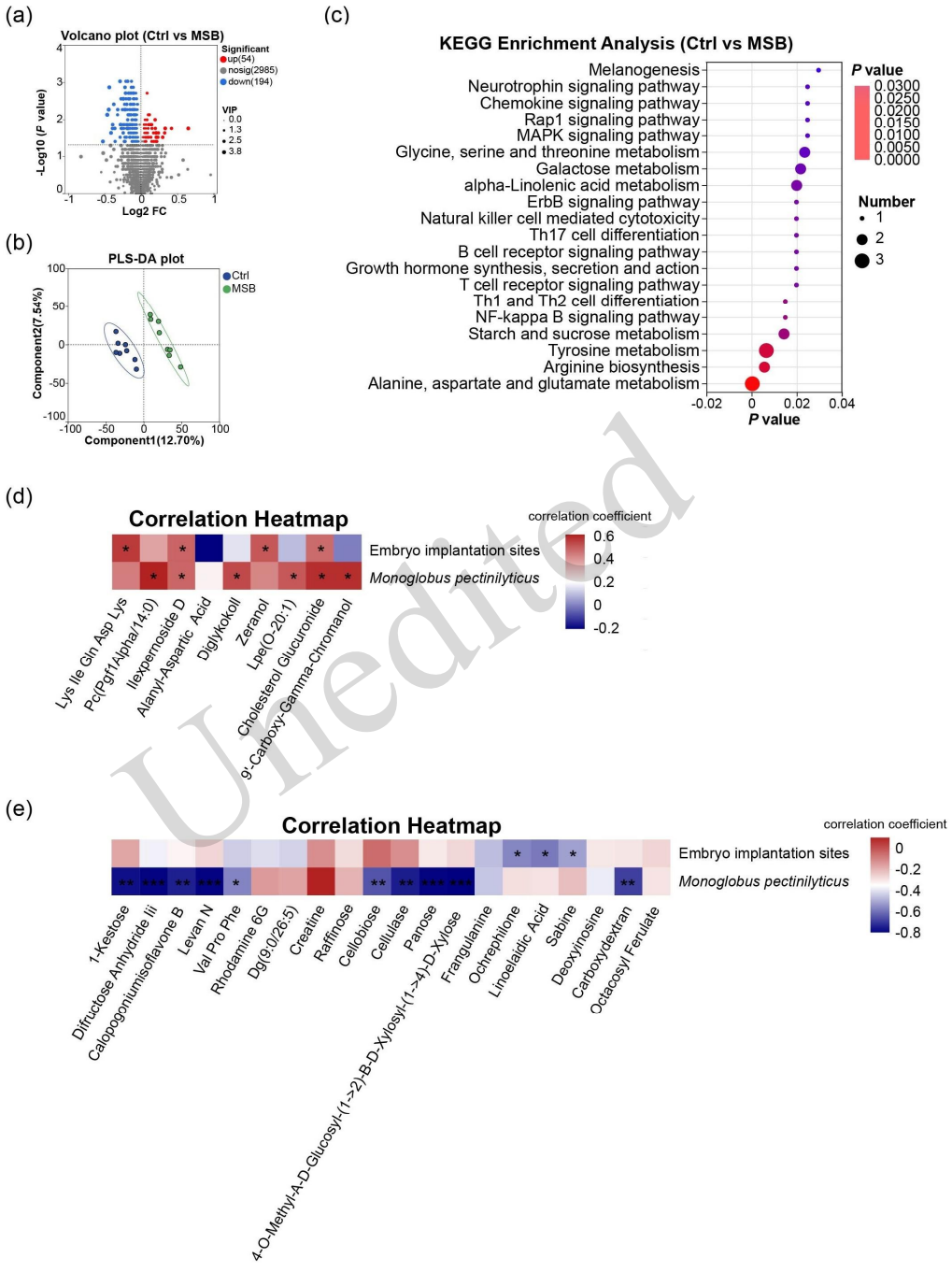

Fig. 6 SB alters the gut metabolome and correlates with implantation success in mice. (a–b) Volcano plot and PLS-DA analysis of colonic metabolome of mice at GD6. (c) KEGG enrichment analysis. (d–e) Correlating the abundance of up- and down-regulated metabolites with embryo implantation sites and *M. pectinilyticus*. Spearman's correlation coefficient (r) is shown. Red, positive correlation; blue, negative correlation. Color intensity reflects |r|. $P<0.05$ for all displayed correlations. PLS-DA, partial least squares discrimination analysis.

Correlation analysis identified associations among differential metabolites, microbial taxa, and embryo implantation sites. Several upregulated metabolites showed positive correlations with both the abundance of *M. pectinilyticus* and the number of embryo implantation sites, while some downregulated metabolites showed negative correlations with these parameters (Figs 6d and 6e).

3.6 SB-induecd modulation of the host serum metabolome in mice

Given the critical role of systemic metabolism in regulating gene expression and physiological homeostasis, we analyzed serum metabolite profiles following SB supplementation. Comparative analysis identified 95 upregulated and 84 downregulated metabolites in the MSB group compared to the Ctrl group (Fig. 7a). All significantly changed metabolites in mice serum are shown in Table S4, including their m/z, retention time, level, and *P* values. The PCA plot shows that the metabolic pattern of the MSB group was significantly different to that of the Ctrl group (Fig. 7b). Significant alterations were observed in specific metabolites, including an increase in arachidonic acid (AA) (Fig. 7c) and a decrease in prostaglandin F2α (PGF2α) (Fig. 7d). KEGG enrichment analysis of serum metabolites highlighted pathways including oxytocin signaling, ovarian steroidogenesis, and the GnRH signaling pathway (Fig. 7e). Correlation analysis showed that 9(Z),11(E)-conjugated linoleic acid and estrane were positively correlated with implantation sites, while phomopsin A and 17-beta-estradiol-3-glucuronide showed negative associations (Figs 7f and 7g).

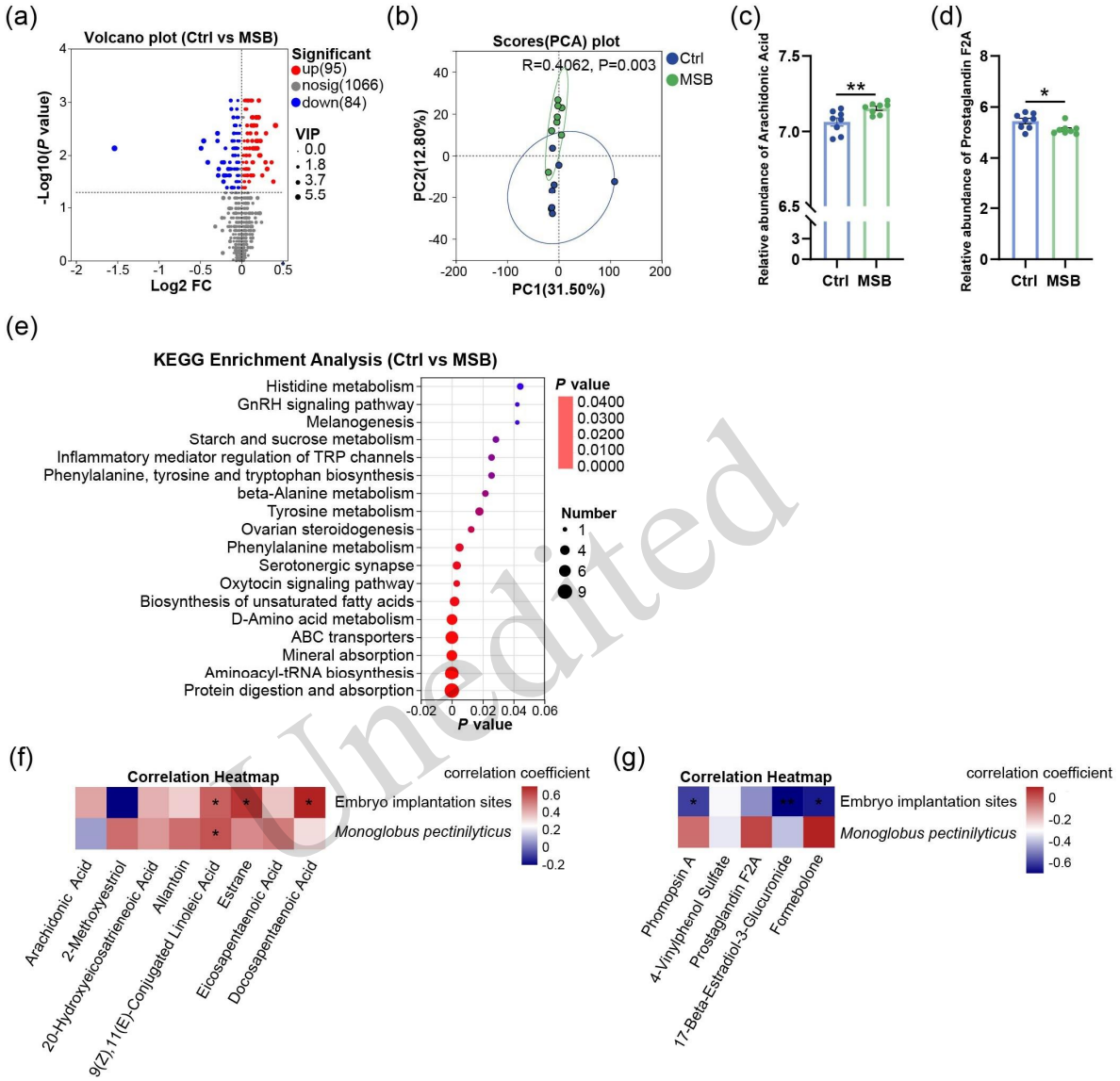

Fig. 7 SB modulates host serum metabolism in mice. (a–b) Volcano plot and PCA plot of serum metabolome of mice at GD6. (c–d) Levels of arachidonic acid and prostaglandin F2A in serum of mice at GD6. (e) KEGG enrichment analysis. (f–g) Correlation analysis. The data are presented as mean±SEM (Ctrl group, n=9; LSB group, n=13; MSB group, n=10; HSB group, n=13). **P*<0.05 and ***P*<0.01 by Student's *t*-test. PCA, principal component analysis.

3.7 SB-induced uterine transcription alterations and their association with enhanced endometrial receptivity in mice

To characterize the uterine transcriptional profile following SB supplementation, we performed transcriptome analysis of uterine tissues. Samples from the two groups formed distinct clusters in both the correlation heatmap and PCA plot, indicating a significant shift in the overall transcriptional profile following SB treatment (Figs 8a and 8b). Differential expression analysis identified 323 significantly upregulated and 370 downregulated genes in the MSB group compared to the Ctrl group (Fig. 8c).

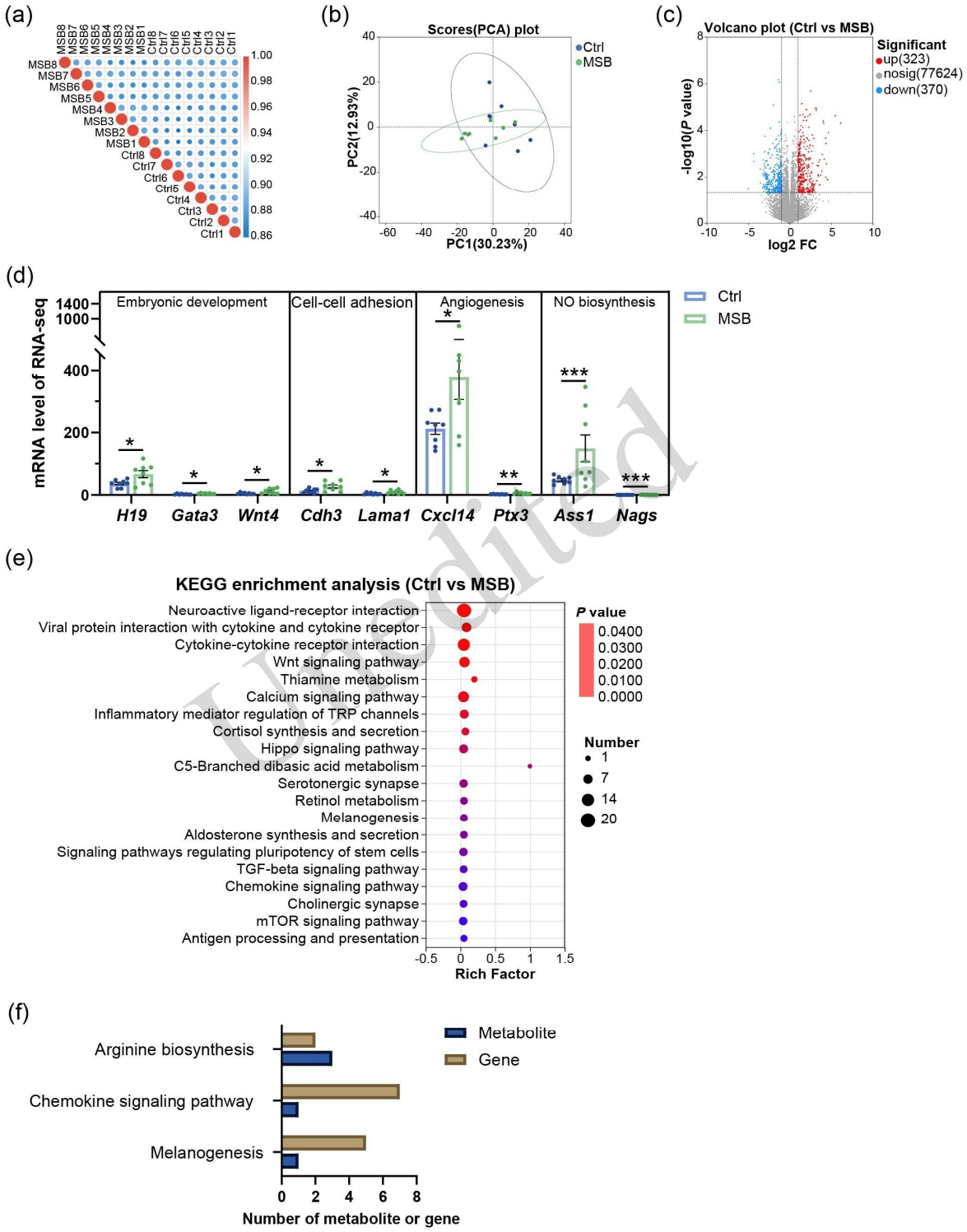

Fig. 8 SB alters uterine transcription and is associated with enhanced endometrial receptivity in mice. (a) Samples correlation heatmap. (b–c) PCA and volcano plot of mice uterine transcriptomics. (d) Bar plot showing mRNA level of genes related to embryonic development, cell-cell adhesion, angiogenesis and NO biosynthesis. (e) KEGG enrichment analysis. (f) KEGG pathways for serum metabolome (blue bar) and uterine transcriptome (brown bar) of mice at GD6. The data are presented as mean±SEM (Ctrl group, n=9; LSB group, n=13; MSB group, n=10; HSB group, n=13). **P*<0.05 and ****P*<0.001 by Student's *t*-test. PCA, principal component analysis.

Among the differentially expressed genes (DEGs), we observed a significant upregulation of several genes known to be involved in embryonic development, cell-cell adhesion, angiogenesis and NO biosynthesis. These included the paternally imprinted gene H19, trophoblast regulator Gata3, uterine gland development factor Wnt4, cell adhesion molecules Cdh3 and Lama1, chemokine Cxcl14, inflammatory regulator Ptx3, and metabolic enzymes Ass1 and Nags (Fig. 8d).

KEGG pathway enrichment analysis of the DEGs revealed significant enrichment of several signaling pathways, including the TGF-beta signaling pathway, aldosterone synthesis and secretion, serotonergic synapse, cortisol synthesis and secretion, and Wnt signaling pathways (Fig. 8e). Furthermore, integrative analysis of the serum metabolome and uterine transcriptome revealed several co-enriched pathways, including arginine biosynthesis, chemokine signaling and melanogenesis (Fig. 8f).

3.8 SB-induced alteration of the uterine proteomic landscape in mice

To further investigate the impact of SB at the protein level, we conducted a quantitative proteomic analysis of uterine tissues. The analysis identified a significant number of proteins that differed in abundance between the MSB and Ctrl groups (Fig. 9a). The protein groups showing significant changes in the mice uterus are listed in Table S5, which includes protein names and corresponding *P* values. PLS-DA showed a clear separation of the proteomic profiles between the Ctrl and MSB groups (Fig. 9b). The treatment groups showed a significant decrease in uterine Wnt4 relative to the Ctrl group (Fig. 9c). Upregulated proteins were enriched in the GnRH signaling pathway, whereas downregulated proteins were enriched in the Renin-angiotensin system, Wnt signaling pathway, and arginine biosynthesis pathway (Figs 9d and 9e). Finally, a PPI network was constructed using the DEPs identified from the enriched pathways in the preceding analysis (Fig. 9f).

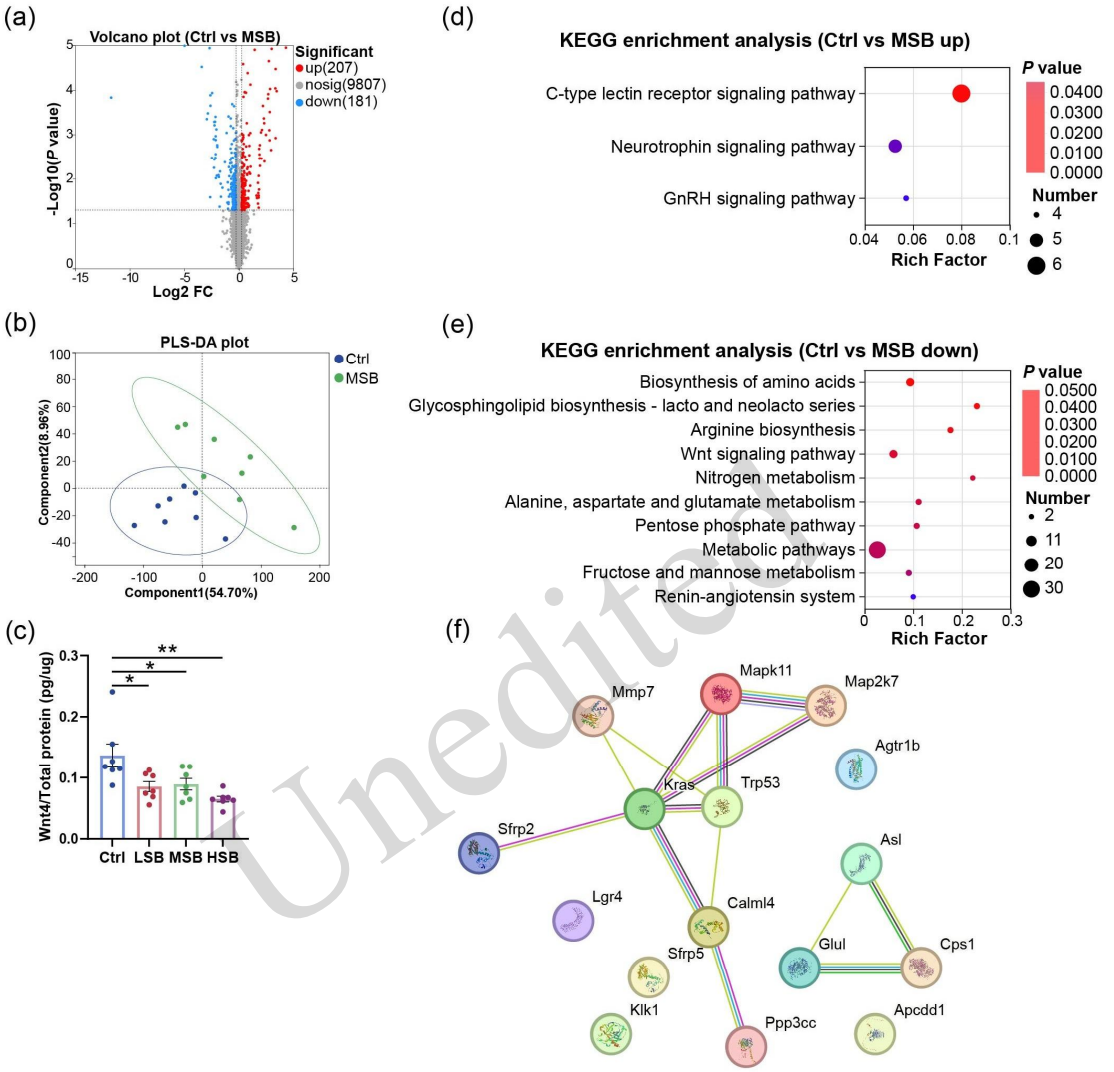

Fig. 9 SB alters the uterine proteomic landscape in mice. (a–b) Volcano plot and PLS-DA plot. (c) The concentration of Wnt4 in uterine tissue. (d–e) KEGG enrichment analysis of up- and down-regulated differential proteins. (f) PPI network analysis. The data are presented as mean±SEM (Ctrl group, n=9; LSB group, n=13; MSB group, n=10; HSB group, n=13). **P*<0.05 and ***P*<0.01 by Student's *t*-test. PLS-DA, partial least squares discrimination analysis.

In summary, these data provide a comprehensive multi-omics characterization of the reproductive and systemic molecular changes associated with dietary SB supplementation.

4 Discussion

Reproductive success is inextricably linked to maternal nutritional status, yet early embryonic loss remains a primary constraint on litter size in livestock production and a significant challenge in human fertility (Cha et al., 2012; Norwitz et al., 2001; Geisert et al., 2002). While genetic selection and superovulation strategies have been explored, their efficacy is limited by low heritability and potential for uterine crowding, respectively (Town et al., 2005; Shi et al., 2025). Consequently, nutritional interventions that enhance endometrial

receptivity and embryo survival offer a more practical and potent approach. This study provides compelling, multi-species evidence that dietary SB supplementation during early gestation correlates with improved reproductive outcomes. However, while the findings suggest a complex interplay between the gut microbiota and the uterus, formal causality remains to be established.

4.1 Association between SB-enhanced reproductive performance and gut microbiota changes

Our main finding is that SB supplementation during the critical peri-implantation period significantly enhances reproductive performance across species. In sows, this manifested as increased litter size at farrowing, while in mice, it directly elevated the number of embryo implantation sites (Figs 1b–1d, Figs 4b and 4c). The effect of SB supplementation on litter size in sows was modest, with an increase of about one piglet per litter in the LSB group, and a clear dose-response relationship was not observed. This may be attributed to the high baseline reproductive performance of the sows in this study, potentially creating a ceiling effect that limits further improvement. Specifically, Chen et al. (2019) used a dietary concentration of 1 g/kg SB (identical to our MSB group) and reported no significant differences in the number of piglets born or born alive, although maternal recovery was significantly improved through a shortened weaning-estrus interval. Lu et al. (2025) showed that a higher concentration of 2 g/kg SB (matching our HSB group) was required to significantly enhance placental efficiency and lactation feed intake, which subsequently supported a trend toward increased total litter size. These data suggest that different concentrations may result in distinct physiological outcomes. In contrast, a more pronounced effect was observed in mice, particularly in the MSB group. However, as noted in the sow trial, the lack of a linear dose-response across all parameters suggests that SB-associated effects may involve non-monotonic biological responses or be influenced by the high baseline performance of the animals. This species-specific difference likely reflects variations in gut physiology, metabolism, and the dynamics of the reproductive tract environment between livestock and rodents. Nevertheless, the consistency of this effect underscores a conserved physiological response associated with SB supplementation across species. Intriguingly, these profound reproductive benefits occurred without significant alterations in systemic levels of major reproductive hormones (estradiol and progesterone) or in total fecal SCFA concentrations (Figs 1e–1g) (Edwards et al., 2005). This critical negative finding suggests that the impact of SB involves more than a simple systemic endocrine or energy-substrate effect.

We did observe correlations that are consistent with a possible role for gut microbiota modulation. However, it is important to recognize that SB can also be directly absorbed from the gut, and its well-known pharmacological actions as an HDAC inhibitor and NF-κB modulator provide a plausible alternative pathway that could directly influence the uterine transcriptome and proteome (Daly et al., 2006). Therefore, the improved reproductive outcomes observed in this study likely reflect parallel responses to systemic SB exposure, involving both direct pharmacological actions of SB on host tissues and co-occurring shifts in the microbial environment.

4.2 SB-associated shifts in gut microbial ecology and their functional implications

Our data show that SB is associated with selective alterations in the maternal gut microbiota, which are closely associated with its early effects. In both sows and mice, SB induced a time-dependent shift in microbial community structure, characterized by the specific enrichment of key bacterial taxa (Figs 2q and 2r, Figs 5l and 5m). Notably, SB supplementation also led to a decrease in alpha diversity coupled with an increase in the Simpson index, indicating reduced species richness and a shift toward dominance of specific taxa. While reduced diversity is often interpreted as a sign of dysbiosis, in this context it is more consistent with a model involving selective modulation of the gut microbiota rather than a deleterious change (Cao et al., 2018). Supporting this interpretation, the enriched taxa included beneficial and metabolically specialized bacteria.

In sows, a striking time-dependent pattern was observed. At GD14, SB-treated sows exhibited a significant reduction in alpha diversity indices (Observed species, Chao, Ace, and Shannon) compared to the Ctrl (Figs 2a–d). This suggests that by early gestation, SB has already induced a shift toward a less diverse but

more functionally specialized microbial community. Interestingly, by GD28, these differences were less pronounced (Figs 2g–j), indicating a partial recovery or stabilization of the microbiota as gestation progressed. One possible explanation is that the initial selective pressure exerted by SB is strongest during the early gestation period, when the gut environment is actively adapting to the intervention. Over time, the microbiota may reach a new equilibrium, with diversity indices returning toward baseline while the functional capacity (e.g., butyrate production, pectin fermentation) remains enhanced (Trevelline et al., 2023). This pattern aligns with the gradual nature of microbial shifts described above and may explain why reproductive benefits (e.g., increased litter size) were observed even when later-gestation physiological markers appeared stable.

The marked increase in *M. pectinilyticus* in mice is particularly noteworthy (Figs 5l and 5m). As a specialized pectin-fermenting bacterium, its enrichment implies that SB fosters a metabolic niche favoring microbes capable of degrading complex polysaccharides (Kim et al., 2017). The parallel enrichment of Streptococcus in both species further highlights a conserved microbial response to SB. While often associated with pathogenesis, many commensal *Streptococcus* species are now recognized for their roles in producing neurotransmitters and immunomodulatory molecules, serving as potential markers that parallel the systemic physiological shifts observed in both the gut and uterine environments. (Rutsch et al., 2020). Additionally, the enrichment of butyrate-producing genera such as *Monoglobus* and known probiotic genera including *Lactobacillus* and *Bifidobacterium* suggests that the microbial community is selectively shaped to favor taxa with specific metabolic capabilities. While these microbial shifts are robustly associated with improved outcomes, it is plausible that they represent one component of a broader systemic response to SB.

4.3 Metabolic profiling: characterization of microbial and systemic variations

The SB-associated shifts in the gut microbiota correspond to substantial changes in the host metabolome. In the gut, this was marked by the significant enrichment of the arginine biosynthesis pathway (Fig. 6c). This finding has direct physiological relevance, as L-arginine is the sole precursor for nitric oxide (NO) (Cooke et al., 2002), a potent vasodilator critical for increasing uterine blood flow during implantation (Madsen et al., 2017). Given that enhanced uterine perfusion is a well-established factor for improving pregnancy outcomes, and that direct dietary arginine supplementation is shown to increase litter size in sows (Wu et al., 2013), our results show that SB supplementation is associated with the enrichment of arginine-related pathways in the gut.

The observed local gut metabolic shift was accompanied by corresponding changes in the systemic circulation, characterized by a distinct serum metabolomic profile (Fig. 7). The coordinated increase in AA and decrease in PGF2α is particularly compelling (Figs 7c and 7d). While AA is a precursor for both pro-inflammatory (e.g., PGF2α) and anti-inflammatory eicosanoids, its elevated pool availability, when processed within a favorably modulated endocrine environment, can be channeled towards pathways that support implantation (Satoh-Asahara et al., 2012). Conversely, the significant decrease in PGF2α (Fig. 7d), a potent luteolysin and stimulant of uterine contractions, is a pivotal finding. This reduction creates a dual benefit by protecting the corpus luteum from premature regression, thereby sustaining progesterone production, and promoting uterine quiescence during the critical period of embryo attachment (Ka et al., 2018). This eicosanoid profile is highly conducive to pregnancy, as it promotes uterine quiescence and supports corpus luteum function, both essential for successful implantation and pregnancy maintenance (Crawford et al., 2023; Basu et al., 2007). These findings reveal a coordinated shift in systemic signaling, creating a pro-gestational metabolic environment that coincides with the altered gut profile.

KEGG pathway enrichment analysis of the serum metabolome further highlighted three key reproductive pathways: oxytocin signaling, ovarian steroidogenesis, and GnRH signaling (Fig. 7e). The enrichment of the oxytocin signaling pathway points to a direct impact on uterine function. Oxytocin is a key regulator of uterine contractility and prostaglandin synthesis (Giannoulias et al., 2002). The precise timing and magnitude of prostaglandin signaling are critical for uterine receptivity and the window of implantation (Cha and Dey, 2014). The modulation of this pathway is associated with adjustments in the uterine environment, potentially suppressing excessive contractions during embryo attachment for successful implantation. Simultaneously, the

enrichment of ovarian steroidogenesis is consistent with the SB-associated changes in systemic metabolic profiles and the synthesis of steroid hormones. The balanced production of estrogen and progesterone from the ovaries is the cornerstone of endometrial preparation. The enrichment of the GnRH signaling pathway represents a fundamental finding. Furthermore, as the master switch of the hypothalamic-pituitary-gonadal (HPG) axis, GnRH triggers the pulsatile release of luteinizing hormone (LH) and follicle-stimulating hormone (FSH). The observed alterations in this pathway parallel the shifts in the reproductive environment, reflecting a molecular landscape that is associated with improved implantation outcomes. This likely leads to a more optimized hormonal milieu for ovulation and, crucially, for the preparation of the corpus luteum and the subsequent production of progesterone, which is indispensable for establishing and maintaining pregnancy (Sparaco et al., 2023).

4.4 Integrated profiling of uterine responses to SB

Ultimately, the systemic signals converge on the uterus, molecularly priming it for implantation. Our transcriptomic data revealed the upregulation of a suite of implantation-critical genes, including H19, Gata3 and Wnt4 (Fig. 8d). These genes govern key processes from placental development and trophoblast invasion to endometrial differentiation and physical cell-cell adhesion, collectively forming a molecular signature of a hyper-receptive state (Gonzalez-Rodriguez et al., 2016; Mi et al., 2000; Pujol Gualdo et al., 2025).

Integrating transcriptomic and proteomic data uncovered an additional layer of sophisticated, time- sensitive regulation. Notably, while components of the Wnt signaling pathway were transcriptionally upregulated (Fig. 8d) their corresponding protein levels were downregulated in the proteome (Fig. 9c). This is unlikely to be a contradiction. Instead, it likely reflects a crucial, temporally precise regulatory mechanism. The timely cessation of endometrial proliferation is essential to initiate its transition to a differentiated and adhesive state, thereby opening the implantation window, which is the discrete period of maximal endometrial receptivity for blastocyst attachment (Ma et al., 2003; Paria et al., 1993). The observed divergence between Wnt-related mRNA and protein levels highlights the complexity of the uterine molecular response. While such patterns may reflect post-translational modifications or temporal shifts in endometrial differentiation, they mainly illustrate the multi-level alterations associated with SB supplementation. Furthermore, the proteomic downregulation of the local renin-angiotensin system and specific glycosphingolipid pathways likely contribute to this pro-receptive state by promoting uterine vasodilation and modulating the local immune environment (Fig. 9d).

4.5 The molecular profile of SB supplementation: a multi-omics perspective

We have provided a comprehensive multi-omics characterization of the molecular changes associated with SB supplementation. Our findings revealed concurrent but distinct alterations across the gut microbiota, systemic metabolome, and uterine transcriptome/proteome. These parallel responses collectively describe a biological state associated with improved embryo implantation and litter size.

However, several limitations must be acknowledged. Uterine tissue metabolomics was not performed, preventing us from directly linking serum metabolite changes to endometrial uptake and downstream signaling. Furthermore, extending future evaluations across the complete gestation and lactation period would provide a more comprehensive understanding of the sustained nutritional benefits of SB on overall sow productivity and offspring development. Nonetheless, this work provides a comprehensive multi-omics dataset and a foundation for future investigations into the associations between systemic molecular shifts and reproductive outcomes associated with SB supplementation.

5 Conclusions

Taken together, our findings suggest that dietary SB supplementation during early gestation could increase litter size in sows and enhance embryo implantation sites in mice. These beneficial effects occurred in association with the simultaneous modification of the gut microbiota, colonic and serum metabolome, and

uterine transcriptome/proteome, highlighting SB as a potential nutritional intervention to improve reproductive outcomes across species. However, the underlying mechanisms require further validation through complementary approaches.

Data availability statement

The 16S rRNA sequencing data have been deposited into the Sequence Read Archive (SRA) database and can be accessed at https://www.ncbi.nlm.nih.gov/bioproject/PRJNA1387164 and https://www.ncbi.nlm.nih.gov/bioproject/PRJNA1389710, respectively. Other research data can be obtained from the authors upon reasonable request.

Acknowledgments

This work was supported by the National Natural Science Foundation of China (Nos. 32230099, 31925037, 32202700, and 32573244).

Author contributions

Xianghua YAN, Qianhong YE and Yuwen CHEN conceived and designed the experiments. Yuwen CHEN wrote and edited the manuscript. Yuwen CHEN, Xiaojian XU and Zhenhong YAN performed the experiments. All authors read and approved the final manuscript and, therefore, had full access to all the data in the study and take responsibility for the integrity and security of the data.

Compliance with ethics guidelines

Yuwen CHEN, Xiaojian XU, Zhenhong YAN, Qianhong YE, Xianghua YAN declare that they have no conflict of interest.

All experimental procedures involving sows and mice were conducted in accordance with guidelines approved by the Institutional Animal Care and Use Committee of Huazhong Agricultural University, Wuhan, China, with approval numbers HZAUSW-2023-0064 and HZAUMO-2025-0282, respectively.

Declaration on the use of generative AI tools

No generative AI tools were used in the preparation of this manuscript.

References

Achache H, Revel A, 2006. Endometrial receptivity markers, the journey to successful embryo implantation. *Hum Reprod Update*, 12(6):731-46. https://doi.org/10.1093/humupd/dml004

Basu S, 2007. Novel cyclooxygenase-catalyzed bioactive prostaglandin F2alpha from physiology to new principles in inflammation. *Med Res Rev*, 27(4):435-68. https://doi.org/10.1002/med.20098

Cao Y, Wu KN, Mehta R, et al., 2018. Long-term use of antibiotics and risk of colorectal adenoma. *Gut*, 67(4): 672-678. https://doi.org/10.1136/gutjnl-2016-313413

Cha J, Dey SK, 2014. Cadence of procreation: orchestrating embryo-uterine interactions. *Semin Cell Dev Biol*, 34:56-64. https://doi.org/10.1016/j.semcdb.2014.05.005

Cha J, Sun XF, Dey SK, 2012. Mechanisms of implantation: strategies for successful pregnancy. *Nat Med*, 18(12):1754-67. https://doi.org/10.1038/nm.3012

Chen JC, Xu QQ, Li YX, et al., 2019. Comparative effects of dietary supplementations with sodium butyrate, medium-chain fatty acids, and n-3 polyunsaturated fatty acids in late pregnancy and lactation on the reproductive performance of sows and growth performance of suckling piglets. *J Anim Sci*, 97(10):4256-4267. https://doi.org/10.1093/jas/skz284

Cooke JP, Losordo DW, 2002. Nitric oxide and angiogenesis. *Circulation*, 105(18):2133-5. https://doi.org/10.1161/01.cir.0000014928.45119.73

Crawford MA, Sinclair AJ, Hall B, et al., 2023. The imperative of arachidonic acid in early human development. *Prog Lipid Res*, 91:101222.

https://doi.org/10.1016/j.plipres.2023.101222
Dalile B, Van Oudenhove L, Vervliet B, et al., 2019. The role of short-chain fatty acids in microbiota-gut-brain communication. *Nat Rev Gastroenterol Hepatol*, 16(8):461-478.
https://doi.org/10.1038/s41575-019-0157-3
Daly K, Shirazi-Beechey SP, 2006. Microarray analysis of butyrate regulated genes in colonic epithelial cells. *DNA Cell Biol*, 25(1):49-62.
https://doi.org/10.1089/dna.2006.25.49
de Lazari MGT, Pereira LX, Orellano LAA, et al., 2020. Sodium butyrate downregulates implant-induced inflammation in mice. *Inflammation*, 43(4):1259-1268.
https://doi.org/10.1007/s10753-020-01205-0
Dey SK, Lim H, Das SK, et al., 2004. Molecular cues to implantation. *Endocr Rev*, 25(3):341-73.
https://doi.org/10.1210/er.2003-0020
Dou XJ, Gao N, Lan J, et al., 2020. TLR2/EGFR are two sensors for pBD3 and pEP2C induction by sodium butyrate independent of HDAC inhibition. *J Agric Food Chem*, 68(2):512-522.
https://doi.org/10.1021/acs.jafc.9b06569
Edwards DP, 2005. Regulation of signal transduction pathways by estrogen and progesterone. *Annu Rev Physiol*, 67:335-76.
https://doi.org/10.1146/annurev.physiol.67.040403.120151
Fellows R, Denizot J, Stellato C, et al., 2018. Microbiota derived short chain fatty acids promote histone crotonylation in the colon through histone deacetylases. *Nat Commun*, 9(1):105.
https://doi.org/10.1038/s41467-017-02651-5
Geisert RD, Schmitt RA, 2002. Early embryonic survival in the pig: Can it be improved? *J Anim Sci*, 80(1): 54-65.
https://doi.org/10.2527/animalsci2002.0021881200800ES10009x
Giannoulias D, Patel FA, Holloway AC, et al., 2002. Differential changes in 15-hydroxyprostaglandin dehydrogenase and prostaglandin H synthase (types I and II) in human pregnant myometrium. *J Clin Endocrinol Metab*, 87(3):1345-1352.
https://doi.org/10.1210/jcem.87.3.8317
Gonzalez-Rodriguez P, Cantu J, O'Neil D, et al., 2016. Alterations in expression of imprinted genes from the H19/IGF2 loci in a multigenerational model of intrauterine growth restriction (IUGR). *Am J Obstet Gynecol*, 214(5):625.e1-625.e11.
https://doi.org/10.1016/j.ajog.2016.01.194
Han C, Shi CP, Liu LM, et al., 2024. Majorbio Cloud 2024: Update single-cell and multiomics workflows. *iMeta*, 3(4):e217.
https://doi.org/10.1002/imt2.217
Jia Z, Xiao ZM, Li L, et al., 2016. Simultaneous determination of multi-organic acids in feed acidifier by ion exclusion chromatography. *Trans Chin Soc Agric Eng*, 32(12):303-308.
https://doi.org/10.11975/j.issn.1002-6819.2016.12.043
Johnson RK, Nielsen MK, Casey DS, 1999. Responses in ovulation rate, embryonal survival, and litter traits in swine to 14 generations of selection to increase litter size. *J Anim Sci*, 77(3):541-57.
https://doi.org/10.2527/1999.773541x
Ka H, Seo H, Choi Y, et al., 2018. Endometrial response to conceptus-derived estrogen and interleukin-1β at the time of implantation in pigs. *J Anim Sci Biotechnol*, 9:44.
https://doi.org/10.1186/s40104-018-0259-8
Keefe D, Kumar M, Kalmbach K, 2015. Oocyte competency is the key to embryo potential. *Fertil Steril*, 103(2):317-22.
https://doi.org/10.1016/j.fertnstert.2014.12.115
Kim CC, Kelly WJ, Patchett ML, et al., 2017. Monoglobus pectinilyticus gen. nov., sp. nov., a pectinolytic bacterium isolated from human faeces. *Int J Syst Evol Microbiol*, 67(12):4992-4998.
https://doi.org/10.1099/ijsem.0.002395
Kimura I, Miyamoto J, Ohue-Kitano R, et al., 2020. Maternal gut microbiota in pregnancy influences offspring metabolic phenotype in mice. *Science*, 367(6481):eaaw8429.
https://doi.org/10.1126/science.aaw8429
Koh A, De Vadder F, Kovatcheva-Datchary P, et al., 2016. From dietary fiber to host physiology: Short-Chain Fatty Acids as key bacterial metabolites. *Cell*, 165(6):1332-1345.
https://doi.org/10.1016/j.cell.2016.05.041
Lin Y, Fang ZF, Che LQ, et al., 2014. Use of sodium butyrate as an alternative to dietary fiber: effects on the embryonic development and anti-oxidative capacity of rats. *PLoS One*, 9(5):e97838.
https://doi.org/10.1371/journal.pone.0097838
Lu CL, Fang ZF, Che LQ, et al., 2025. Dietary sodium butyrate supplementation during mid-to-late gestation enhances reproductive performance and antioxidant capability in sows. *Animal*, 19(5):101516.
https://doi.org/10.1016/j.animal.2025.101516

Ma WG, Song H, Das SK, et al., 2003. Estrogen is a critical determinant that specifies the duration of the window of uterine receptivity for implantation. *Proc Natl Acad Sci U S A*, 100(5):2963-8. https://doi.org/10.1073/pnas.0530162100

Madsen JG, Pardo C, Kreuzer M, et al., 2017. Impact of dietary l-arginine supply during early gestation on myofiber development in newborn pigs exposed to intra-uterine crowding. *J Anim Sci Biotechnol*, 8:58. https://doi.org/10.1186/s40104-017-0188-y

Mi S, Lee X, Li X, et al., 2000. Syncytin is a captive retroviral envelope protein involved in human placental morphogenesis. *Nature*, 403(6771):785-9. https://doi.org/10.1038/35001608

Mumford SL, Chavarro JE, Zhang CL, et al., 2016. Dietary fat intake and reproductive hormone concentrations and ovulation in regularly menstruating women. *Am J Clin Nutr*, 103(3):868-77. https://doi.org/10.3945/ajcn.115.119321

Munoz-Suano A, Hamilton AB, Betz AG, 2011. Gimme shelter: the immune system during pregnancy. *Immunol Rev*, 241(1):20-38. https://doi.org/10.1111/j.1600-065X.2011.01002.x

Norwitz ER, Schust DJ, Fisher SJ, 2001. Implantation and the survival of early pregnancy. *N Engl J Med*, 345(19):1400-8. https://doi.org/10.1056/NEJMra000763

Paria BC, Huet-Hudson YM, Dey SK, 1993. Blastocyst's state of activity determines the "window" of implantation in the receptive mouse uterus. *Proc Natl Acad Sci U S A*, 90(21):10159-62. https://doi.org/10.1073/pnas.90.21.10159

Pujol Gualdo N, Džigurski J, Rukins V, et al., 2025. Atlas of genetic and phenotypic associations across 42 female reproductive health diagnoses. *Nat Med*, 31(5):1626-1634. https://doi.org/10.1038/s41591-025-03543-8

Quivy V, Van Lint C, 2004. Regulation at multiple levels of NF-kappaB-mediated transactivation by protein acetylation. *Biochem Pharmacol*, 68(6):1221-9. https://doi.org/10.1016/j.bcp.2004.05.039

Red-Horse K, Zhou Y, Genbacev O, et al., 2004. Trophoblast differentiation during embryo implantation and formation of the maternal-fetal interface. *J Clin Invest*, 114(6):744-54. https://doi.org/10.1172/JCI22991

Ren Y, Yu G, Shi CP, et al., 2022. Majorbio Cloud: A one-stop, comprehensive bioinformatic platform for multiomics analyses. *Imeta*, 1(2):e12. https://doi.org/10.1002/imt2.12

Rutsch A, Kantsjö JB, Ronchi F, 2020. The gut-brain axis: how microbiota and host inflammasome influence brain physiology and pathology. *Front Immunol*, 11:604179. https://doi.org/10.3389/fimmu.2020.604179

Satoh-Asahara N, Shimatsu A, Sasaki Y, et al., 2012. Highly purified eicosapentaenoic acid increases interleukin-10 levels of peripheral blood monocytes in obese patients with dyslipidemia. *Diabetes Care*, 35(12): 2631-2639. https://doi.org/10.2337/dc12-0269

Shi L, Hao W, Li Z, et al., 2025. Genome-wide association study and genomic prediction of sow resilience based on reproductive traits. *Animal*, 19(9):101607. https://doi.org/10.1016/j.animal.2025.101607

Sparaco M, Carbone L, Landi D, et al., 2023. Assisted Reproductive Technology and Disease Management in Infertile Women with Multiple Sclerosis. *CNS drugs*, 37(10):849-866. https://doi.org/10.1007/s40263-023-01036-1

Town SC, Patterson JL, Pereira CZ, et al., 2005. Embryonic and fetal development in a commercial dam-line genotype. *Anim Reprod Sci*, 85(3-4):301-16. https://doi.org/10.1016/j.anireprosci.2004.05.019

Trevelline BK, Sprockett D, DeLuca WV, et al., 2023. Convergent remodelling of the gut microbiome is associated with host energetic condition over long-distance migration. *Funct Ecol*, 37(11):2840-2854. https://doi.org/10.1111/1365-2435.14430

Wang HB, Dey SK, 2006. Roadmap to embryo implantation: clues from mouse models. *Nat Rev Genet*, 7(3):185-99. https://doi.org/10.1038/nrg1808

Wu GY, Bazer FW, Satterfield MC, et al., 2013. Impacts of arginine nutrition on embryonic and fetal development in mammals. *Amino Acids*, 45(2):241-56. https://doi.org/10.1007/s00726-013-1515-z

Yamada M, Takanashi K, Hamatani T, et al., 2012. A medium-chain fatty acid as an alternative energy source in mouse

preimplantation development. *Sci Rep*, 2:930.
https://doi.org/10.1038/srep00930

Ye QH, Cai S, Wang S, et al., 2019. Maternal short and medium chain fatty acids supply during early pregnancy improves embryo survival through enhancing progesterone synthesis in rats. *J Nutr Biochem*, 69:98-107.
https://doi.org/10.1016/j.jnutbio.2019.03.015

Ye QH, Hu YF, Jiang HY, et al., 2025. Maternal intestinal L. vaginalis facilitates embryo implantation and survival through enhancing uterine receptivity in sows. *Microbiome*, 13(1):145.
https://doi.org/10.1186/s40168-025-02141-7

Ye QH, Li HY, Xu BY, et al., 2023. Butyrate improves porcine endometrial epithelial cell receptivity via enhancing acetylation of histone H3K9. *Mol Nutr Food Res*, 67(16):e2200703.
https://doi.org/10.1002/mnfr.202200703

Ye XQ, Hama K, Contos JJ, et al., 2005. LPA3-mediated lysophosphatidic acid signalling in embryo implantation and spacing. *Nature*, 435(7038):104-8.
https://doi.org/10.1038/nature03505

Zhang S, Lin HY, Kong SB, et al., 2013. Physiological and molecular determinants of embryo implantation. *Mol Aspects Med*, 34(5):939-80.
https://doi.org/10.1016/j.mam.2012.12.011

Zhao YS, Wang DP, Huang YP, et al., 2021. Maternal butyrate supplementation affects the lipid metabolism and fatty acid composition in the skeletal muscle of offspring piglets. *Anim Nutr*, 7(4):959-966.
https://doi.org/10.1016/j.aninu.2020.11.017

Supplementary information

Tables S1–S5